Rock Mechanics and Rock Engineering (2018) 51:2911–2933
https://doi.org/10.1007/s00603-018-1476-3

ORIGINAL PAPER

Influence of Discontinuities on the Squeezing Intensity in High In Situ Stresses (a Tunnelling Case Study; Actual Evidences and TBM Release Techniques)

Mahdi Rasouli Maleki[1] · **Roohollah Narimani Dehnavi**[2]

Received: 9 September 2017 / Accepted: 2 April 2018 / Published online: 30 April 2018

Abstract
Squeezing rock condition has always been a major concern as one of the principle geological hazards when tunnelling in weak overstressed rock masses. This phenomenon often occurs in shear faulted zones, extremely jointed regions or metamorphic rocks with thin schist layers. Due to the inherent vulnerability of shielded TBMs to jamming, lack of sufficient accurate understanding upon existing squeezing conditions could lead to TBM jamming and long delays in the project duration as a result of TBM downtime and excessive associated costs. In this research, attempts were made to describe the squeezing conditions encountered in July 2014 in the long tunnel of Zagros as a special case study in Iran. The results of the conducted analyses as well as the experiences obtained from this project are presented accordingly. The research procedure in this paper is explained in two separate stages. In the first stage, joint characteristics and mechanical properties of rock mass are estimated, and the behaviour of TBM jamming section of the tunnel is simulated using FLAC and UDEC as the continuous and discontinuous modelling codes. By taking advantage of these simulations and the comparisons, the influence of existing discontinuities and the intensifying effect of overburden stress on the encountered harsh squeezing conditions are analysed accordingly. In the next stage, main reasons and actual indications of TBM jamming that occurred in the squeezing regions of the Zagros Tunnel are investigated. These results are presented in three separate sections including geological indications such as the amount of injected pea gravel and cement grouting as segmental lining backfill materials, field observations regarding the segmental lining and effects on the operational parameters of machine including thrust force, cutterhead torque, Field Penetration Index and the pressure applied by the auxiliary thrust cylinder jacks. Lastly, the most efficient implemented techniques for releasing the machine are explained step by step.

Keywords Squeezing mechanism · Numerical modelling · Tunnel-boring machine (TBM) · Field Penetration Index (FPI) · TBM release strategies · High stresses tunnels

1 Introduction

The overall trend towards long-distance and deep tunnelling by tunnel-boring machines (TBM) has led to tougher geological conditions encountered in numerous projects. These unfavourable ground conditions can significantly affect the TBM performance as a result of underestimating rock mechanics associated problems. However, despite their adverse effects on the overall behaviour of underground structures, appropriate solutions can control these conditions to some extent (Barla and Pelizza 2000).

Depending upon the in situ stress state and the rock mass strength, different behaviours of rock mass including stable and competent or squeezing and failing could be anticipated (Singh and Goel 2006). The squeezing in rocks is regarded as a geological condition leading to large deformations which occur around the tunnel media as a result of high in situ stresses and weak material properties and is known to be a major factor for predicting the rock mass behaviour in underground excavations (Rasouli Maleki 2009). The tunnel wall stability and the extent of convergences around its

✉ Mahdi Rasouli Maleki
Mahdi.Rasouli@yahoo.com

[1] Water & Power Resources Development Co. (IWPCO) and Head of Engineering Geology Department, Harazrah Consulting Engineers Group, Tehran, Iran

[2] Underground Structures Department, Rayab Consulting Engineers Co., Tehran, Iran

perimeter are generally governed by major factors including high deformability, low shear strength, and high in situ stress state. (Mahendra et al. 2007). According to the International Society of Rock Mechanics (ISRM), squeezing is the consequence of time-dependent large deformations taking place around tunnels associated with creep, caused by exceeding a limiting shear stress (Barla 2001). In mechanized tunnelling, adverse effects on the TBM performance as a result of squeezing behaviour of the ground need to be predicted. This process could even question the feasibility of excavation using TBMs, since even a small convergence may lead to shield jamming (Ramoni and Anagnostou 2010a).

Numerical investigations have been conducted to analyse the specific problems associated with mechanized tunnelling in squeezing ground, the occurrence of shield jamming and the effects of countermeasures (Ramoni and Anagnostou 2006, 2010a, b, 2011). More recently, advanced continuous three-dimensional models have also been adopted to assess the ground condition at the tunnel face and the shield–ground interaction for studying the shield-jamming potential (Hasanpour et al. 2014). Several attempts were made to quantify squeezing potential by comparing the rock mass strength with induced stresses (Singh et al. 1992; Goel et al. 1995; Jethwa et al. 1984; Hoek and Marinos 2000a). Panthi and Nilsen (2007) used a combination of the semi-analytical method suggested by Hoek and Marinos (2000b, c) and the empirical formula proposed by Panthi (2006) for Himalayan rock mass conditions. As for the effect of blocky conditions on intensifying possible instabilities and ground convergences, numerical models are the most efficient tools, in case discontinuity properties with acceptable accuracy can be provided. Among numerical methods, discrete modelling techniques have been widely used to simulate tunnelling in blocky grounds by modelling the rock mass as intact rock and joints. (Leitner et al. 2006; Goricki et al. 2005; Ferrero et al. 2004). Detailed parametric studies have revealed the effect of different joint characteristics including orientation and strength properties as well as the influence of in situ stresses on the rock mass behaviour and possible squeezing conditions (Solak 2009).

As stated by Bilgin and Algan (2012), in addition to numerous academic studies, published case studies always help academicians to verify their theoretical work and numerical analysis. Experiences gained through tunnelling projects in squeezing conditions and the countermeasures taken to avoid additional costs pertaining to TBM downtime can significantly prevent difficulties of the similar conditions in other projects (Bilgin and Algan 2012; Shaterpour Mamaghani et al. 2015, Narimani Dehnavi et al. 2016). However, in spite of the extensive conducted investigations on the discontinuous behaviour of blocky grounds, few detailed studies regarding the effect of discontinuities on squeezing behaviour with actual results from case studies have been presented so far. In this research, numerical investigations are carried out to analyse the squeezing conditions of the Zagros Tunnel in blocky grounds. A detailed analysis is conducted on the actual symptoms indicating the onset of squeezing phenomena prior to the occurred TBM jamming. Some of the experiences and employed techniques to release the TBM are also presented in detail.

2 Project Description

The Zagros Tunnel is one of the components of the Garmsiri project in Iran which is planned to transfer water with the capacity of 70 m^3/s from the Sirvan River situated in the Sanandaj province to vast plains of Sare Pole Zahab in the Kermanshah Province. The tunnel is around 49 km long, and its axis is oriented at north-east–south-west. It was primarily introduced in two separate lots of A and B by Iran Water & Power Resources Development Co. (IWPCO). The main aim of constructing this tunnel is to provide the Sare Pole Zahab town with drinking water and transfer the required agricultural water to vast plains in south-western parts of Iran.

Lot B of this tunnel, which is the subject of research in this paper, is 25.7 km in length and 6.73 m in diameter. Each ring of the concrete lining system is divided into 4 hexagonally shaped segments. The tunnel has been excavated by a double-shield TBM manufactured by Herrenknecht. The tunnel axis direction is from south-west to north-east with a positive dip of 0.08%. From a geographical point of view, the inlet portal is 2 km away from the south-eastern part of the Ezgaleh village, and the distance from the outlet portal to the north-western part of the Banilouvan village is approximately 300 m (Rasouli Maleki and Memmarian 2015; Rasouli Maleki 2018a).

This tunnel passes the Emam Hassan, Kordi Ghaseman and Zimkan rivers, and in the rest of the path, it meets lot A of the project in north-east. The maximum overburden of tunnel is 1026 m in the chainage 23 + 300 km starting from outlet portal. The commencement of the project was in March 2006. After excavating an approximate length of 14.5 km, the TBM was totally overhauled in a cavern situated in chainage 14 + 800 km in July 2011. The technical specifications of the TBM are presented in Table 1.

3 Geological Condition

Among different structural categories of Iran, the Zagros Tunnel is located in the Zagros belt. Young tectonic movements of Zagros in this belt have brought about a north-west–south-east and vertical direction in the axis of anticlines and synclines of the area. In general, development of inverse faults and regular folds together with the absence of

Table 1 Main specifications of TBM (Rasouli Maleki 2018b)

Parameter	Value
Total TBM weight (approx.)	573 ton
Bore diameter	6.73 m (with new discs)
Number of disc cutters	42 (34 items single + 4 items double)
Disc diameter	432 mm
Cutterhead speed	0–9.05
Track pitch (vertical area)	90 mm
Drive power (motors)	6 × 350 kW = 2100 kW
Machine torque (nominal)	2104 kNm (nominal load)
Maximum cutterhead thrust	25,722 kN (at 320 bar)
Stroke thrust cylinder	800 mm
Maximum auxiliary thrust	36,397 kN (at ~400 bar)
Stroke auxiliary thrust cylinders	2600 mm

Fig. 1 Geographical location of Zagros Mountains and the project position in Iran

volcanic, plutonic and metamorphic activities are recognized as some of the most important characteristics of this belt. The position of lot B with respect to these folds is such that the tunnel axis is perpendicular to the axis of folds in this region, and the tunnel path intersects the width of anticlines (Fig. 1).

According to geological investigations, it is evident that the general geology of the Zagros Tunnel consists of various types of sedimentary units, including argillaceous limestone, shale and sandstone, being parts of the Ilam, Gourpi and Pabdeh formations. These units belong to Upper Cretaceous and Tertiary sediments and have been deposited in the Zagros sedimentary basin (Rasouli Maleki and Memmarian 2015; Rasouli Maleki and Yousefi Mahmoud 2015).

Based on conducted geological studies, the stratigraphy of lot B of the Zagros Tunnel in the chainage 17 + 500 km to 20 + 000 km can be categorized in four lithological subdivisions:

- JL5 from chainage 17 + 500 km to 18 + 650 km consisting of medium bedded argillaceous limestone with seems of dark grey shale.
- JL4 from chainage 18 + 650 km to 18 + 902 km consisting of medium bedded, dark grey limestone with massive and cliff-forming grey limestone in top and bottom.
- JL3 from chainage 18 + 902 km to 19 + 160 km consisting of thin to medium bedded grey argillaceous limestone.
- JL2 from chainage 19 + 160 km to 20 + 000 km consisting of massive and cliff-forming dark grey limestone.

The longitudinal geological profile together with stratigraphy units of the tunnel is depicted in Fig. 2.

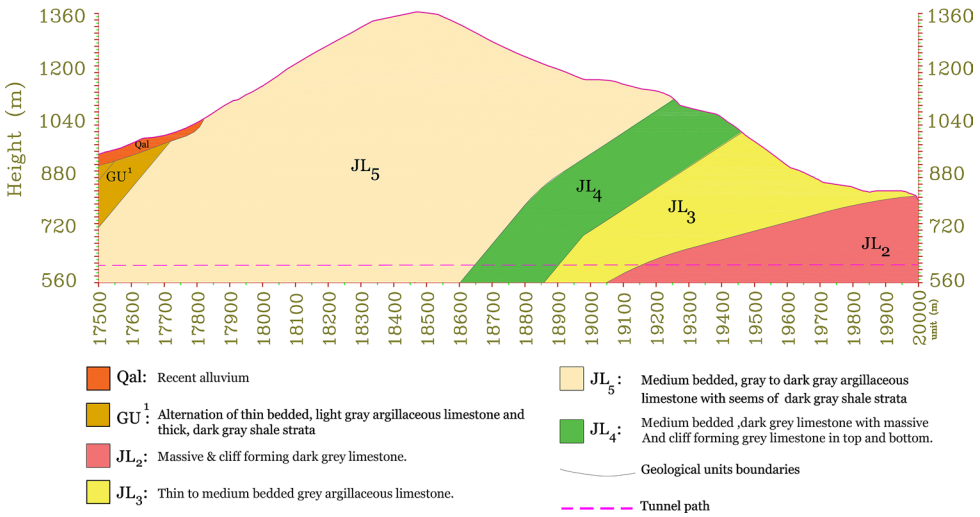

Fig. 2 Geological profile of the Zagros Tunnel (from chainage17 + 500 km to 20 + 000 km)

4 Discontinuity Properties

Structural features of rock masses, including discontinuities, can significantly affect the rock mass properties and its response to tunnelling operations (Rasouli Maleki 2009). In this regard, discontinuity properties including orientation, spacing, persistence, roughness, aperture and infilling were determined based on the ISRM (1981) standards (Rasouli Maleki 2011). Field mappings were carried out to obtain Rosette and pole contour diagrams by using Dips 5.1 software (Rocscience 2002). According to these diagrams indicated in Fig. 3, the dominant joint sets for the rock units along the tunnel are determined. The investigation results prove that the bedding planes are the dominant discontinuities controlling the rock mass behaviour along the tunnel path. The main properties of joint sets in JL5 unit are shown in Table 2.

5 Numerical Modelling of Squeezing Conditions

Squeezing of rock is a process of large deformation which occurs around the tunnel due to stress concentration and material properties, and it is a major factor for predicting rock behaviour in underground excavations (Rasouli Maleki 2009). This hazard is a common phenomenon in poor rock masses under high in situ stress conditions. High deformability, low shear strength and the high in situ stress state are the major factors that govern the tunnel wall stability and the extent of closure (Mahendra et al. 2007).

5.1 Numerical Modelling Process

The orientation and strength properties of discontinuities as well as the existing high in situ stresses around the tunnel section were identified as the main reasons of the encountered harsh geological conditions in the chainage from 18 + 498 km to 18 + 546 km. Therefore, relevant measures were needed to be taken to evaluate the influence of these two main factors. In order to investigate the discontinuous behaviour of blocky grounds, the most

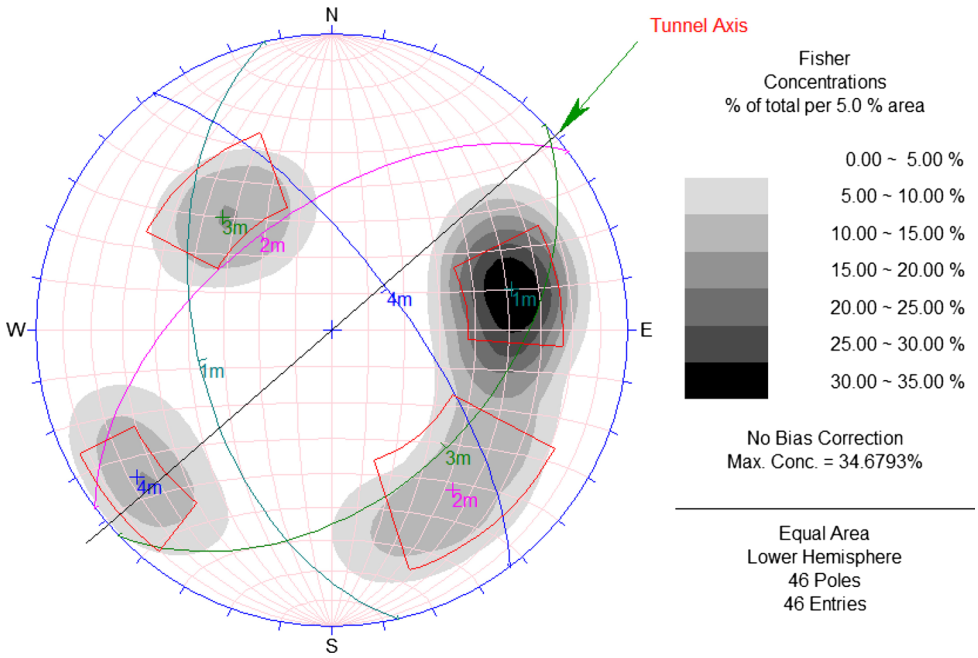

Fig. 3 Rosette diagram and main planes of joint sets in JL5 unit

Table 2 Main properties of joint sets in JL5 unit

Unit	Joint sets	Dip	Dip direction	Spacing (cm)	Aperture (mm)
JL5	Bedding	45–55 (50)	245–275 (260)	140–160 (150)	0.1–0.9 (0.5)
	Jl	55–65 (60)	305–335 (320)	45–65 (55)	6.1–6.9 (6.5)
	J2	35–45 (40)	125–155 (140)	240–260 (250)	5.5–7.5 (6.0)
	J3	70–80 (75)	40–70 (55)	165–185 (175)	6.0–7.0 (6.5)

common tools are analytical and numerical methods. The majority of analytical approaches regarding the blocky behaviour in tunnels have been proposed according to the block theory (Solak 2009). In spite of the improvements made on their main features, they are not suitable for cases where stress-induced failure is the dominating factor (Solak 2009). On the other hand, numerical methods are capable of modelling discontinuities such as joints, faults as well as groundwater conditions, and they can offer more realistic evaluations upon stability of various structures (Stead et al. 2001). Numerical analysis could be made explicitly by employing a discontinuous approach or get simplified by using continuous methods (Maria et al. 2004). Continuous models are more efficient for analysing the stability in rock masses consisting of large volume of intact rocks, weak or severely crushed rocks similar to soil, while discontinuous modelling can be suitable for tunnels in which their stability is controlled by the behaviour of discontinuities (Stead et al. 2001). Among the available discontinuous numerical approaches, the distinct element method (DEM) as an efficient tool can be employed to simulate rock block detachment as well as global and local instability in tunnels, while these conditions cannot be distinguished by continuous approaches (Maria et al. 2004)

In order to investigate the significant effect of discontinuities and in situ stresses on the overall mechanical behaviour in this region, two common numerical codes are employed. The distinct element method (DEM) as the discontinuous numerical approach was applied using UDEC (Universal Distinct Element Code). Rock masses can be modelled by UDEC in form of discrete blocks, with the discontinuities as intersections of them being capable of motion, rotation, and deformation. Additionally, continuous models were generated by finite difference method (FDM) using the FLAC code (Fast Langrangian Analysis of Continua) (Itasca, FLAC2D 2013; Itasca, UDEC 2013). According to the rock mass characteristics and the procedure for creating numerical models which are described in the two following sections, three main model types are established so as to evaluate the role of discontinuities and the existing high in situ stresses around the tunnel. Subsequently, the results obtained from each of the models are compared and discussed accordingly.

5.2 Physical and Mechanical Properties of Rock Mass

In preliminary studies, sufficient site investigations into the physical and mechanical properties of intact rock and discontinuities are necessary to avoid misrepresenting the rock mass features. According to the site observations in this study, the rock mass lithology in the TBM jamming section is identified as argillaceous limestone with interlayers of shale. By conducting laboratory tests on a number of rock samples, the intact rock mechanical parameters were obtained. Among the rock mass properties, determination of shear strength of joint surfaces is an involved process. The values are affected by a number of factors including the type and origin of discontinuities, roughness, depth of weathering, hardness, water condition and the type of infilling material. According to the previous research in this field, the three main parameters that take account of the aforementioned factors include the joint roughness coefficient (JRC), the joint wall compressive strength (JCS) and the basic friction angle of the rock material (Rasouli Maleki 2011).

In this research, by taking advantage of joint mapping studies, site mechanical tests on the joint surfaces (Schmitt Hammer test) and laboratory tests on the acquired rock samples, the main effective parameters in the numerical analysis were calculated by different methods introduced in Rasouli Maleki (2011). The average values of the input joint sets and bedding planes mechanical properties are presented in Table 3, and the mechanical properties of the intact rock and rock mass to be used in UDEC and FLAC are listed in Table 4.

5.3 Model Establishment

For both continuous and discontinuous modelling techniques, a plane strain condition is presumed in -dimensional modelling for tunnelling. As illustrated in the Fig. 4 (left), roller boundary conditions were defined along the

Table 3 Bedding and joint sets plane mechanical properties

Joint sets	Value (min–max, ave.)			
	Bedding	Joint set 1	Joint set 2	Joint set 3
Joint roughness coefficient, JRC	4–6 (5)	6–8 (7)	8–10 (9)	12–14 (13)
Joint compressive strength, JCS (MPa)	10–20 (15)	10–20 (15)	5–15 (10)	5–15 (10)
Cohesion (MPa)	0.22–0.32 (0.27)	0.26–0.49 (0.37)	0.40–0.52 (0.46)	0.61–0.81 (0.71)
Residual friction angle (°)	33–39 (36)	31–37 (34)	28–36 (32)	28–34 (31)
Normal stiffness, kn (GPa/m)	2.3–12.3 (7.3)	2.75–4.95 (3.85)	3–5.8 (4.4)	2.65–5.05 (3.85)
Shear stiffness, ks (GPa/m)	2.2–3 (2.6)	1.71–2.91 (2.31)	1.1–1.9 (1.5)	1.91–2.71 (2.31)

Table 4 Geo-mechanical properties of intact rock and rock mass

Parameter	Value (min–max, ave.)	
	Intact rock (used in UDEC programme)	Rock mass (used in FLAC programme)
Unit weight (ton/m^3)	2.4–2.5 (2.45)	2.4–2.5 (2.45)
Uniaxial compressive strength (MPa)	50–70 (60)	3.36–4.56 (3.96)
Tensile strength (MPa)	3.5–7.5 (5.5)	0.12–0.22 (0.17)
Cohesion (MPa)	7.5–9.9 (8.7)	25.2–33.2 (29.2)
Friction angle (°)	49–61 (55)	1.96–2.16 (2.06)
Modulus of deformation (GPa)	13.2–17.2 (15.2)	2.73–6.73 (4.73)
Poisson's ratio	0.18–0.22 (0.2)	0.21–0.25 (0.23)

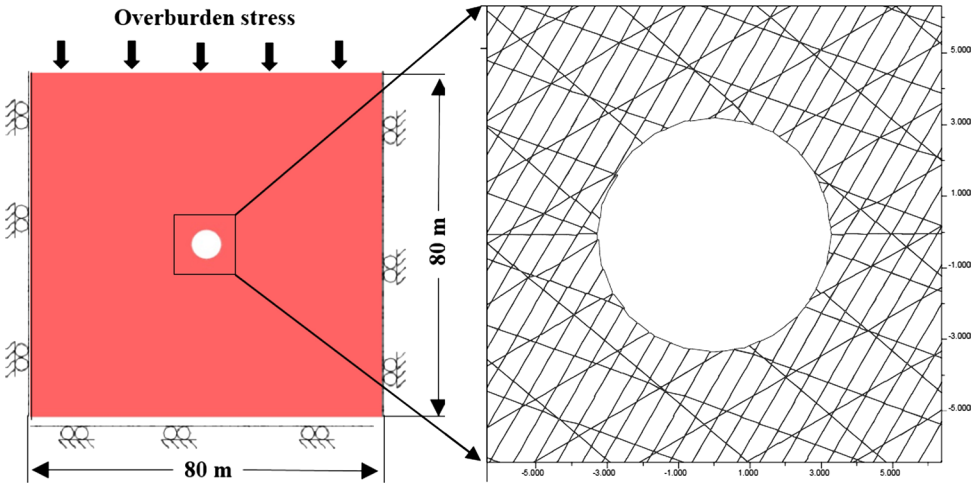

Fig. 4 Boundary condition of the numerical discontinuous models

lateral sides of the models so that no displacement would be allowed in *x* direction. Additionally, at the bottom of the model, the boundary was also considered as a roller boundary such that no movement would be allowed in *y* direction. A domain with 80 m height and 80 m length is defined in the models, and the remaining overburden stress is initialized in the models by applying initial stress to the grids with respect to the overburden. The three joint sets together with the bedding plane intersecting the tunnel perimeter are depicted in Fig. 4 (right). The input dip and dip direction values in the UDEC are the apparent dip and dip direction calculated based on the tunnel axis azimuth which is 49°. As for the continuous model, rectangular meshes with the size of 30 cm are generated.

It should be mentioned that the Mohr–Coulomb criterion is presumed for the intact rock and rock mass properties in UDEC and FLAC, respectively. As for the joint set properties in UDEC, the Coulomb Slip criterion was adopted. Moreover, vertical and horizontal gravitational stresses are considered as in situ stress in the whole model, and the ratio of horizontal to vertical stresses (K_0) is 1.

In the next three subsections, a continuous model, a discontinuous model with the actual overburden(770 m) and two discontinuous models with lower overburdens (100 and 400 m) are created to evaluate the effect of discontinuities as well as the significant influence of high in situ stresses around the tunnel.

5.3.1 Numerical Analysis in Continuous Mode

By neglecting the effect of structural instabilities, a continuous model with the aforementioned geometry and rock mass properties inserted in Table 4 is created in FLAC. After solving the model, stability analysis features including the induced stress magnitudes in *yy* direction with total displacements and the extension of plastic zone around the tunnel are presented in Fig. 5. According to the results, a 3-m-thick plastic zone and a maximum of 5 cm displacement are recorded around the tunnel which obviously does not indicate a major concern regarding squeezing conditions.

5.3.2 Numerical Analysis in Discontinuous Mode with Actual Tunnel Overburden

Unlike the continuous model, three joint sets along with the bedding plane identified in the tunnel perimeter are imported in the DEM model in UDEC, according to the mechanical properties introduced in Tables 3 and 4. By completing the

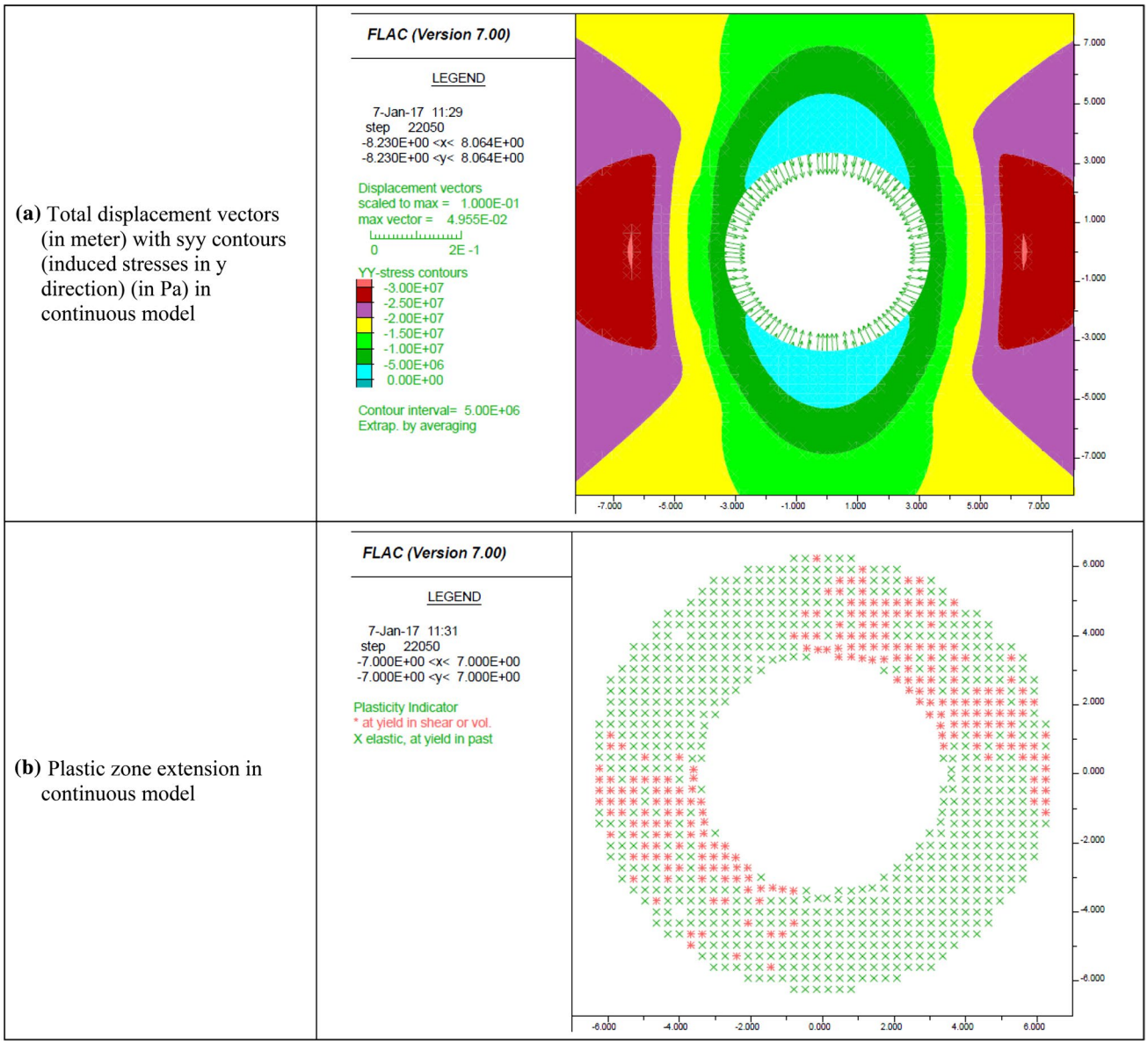

Fig. 5 Total displacements and plastic zone around tunnel based on continuous mode

conducted analysis, major structural instabilities were recognized around the tunnel. As can be seen in Fig. 6a, the displacements around the tunnel in the discontinuous model are in the range of 9–20 cm. Maximum displacements of around 28 cm presenting failed blocks were also recorded in some local regions. Moreover, according to Fig. 6b, the maximum plastic zone thickness is around 3 m in walls. However, the slip surfaces of joints depicted in Fig. 6b by red lines prove a 3.5-m extension zone for slip failures. The induced stresses around tunnel are also indicated as contours in Fig. 6c.

In DEM analyses, displacements measured at the interior boundary of the tunnel cannot be good indicators of the overall behaviour of the tunnel because of localised effects. As stated by Solak (2009), this problem can be solved by determining the average value of displacements in the region at a distance of 2 m from the boundary of the tunnel instead of defining points on the tunnel perimeter. Besides, the shear and tensile failures took place along joints are determined as the failure zone (Solak 2009). By taking account of these facts, the mean value of displacement around the tunnel in discrete analysis would be 13 cm, and the depth of failure is around 3.5 m which is slightly more than the tunnel radius.

In order to study the ground behaviour, a general category with description of the possible failure types during excavation without considering the support system and sequential tunnelling was introduced in (Osterreichische Gesellschaft fur Geomechanik 2001). Afterwards, a delimiting criterion for the quantitative assessment of the ground behaviour was

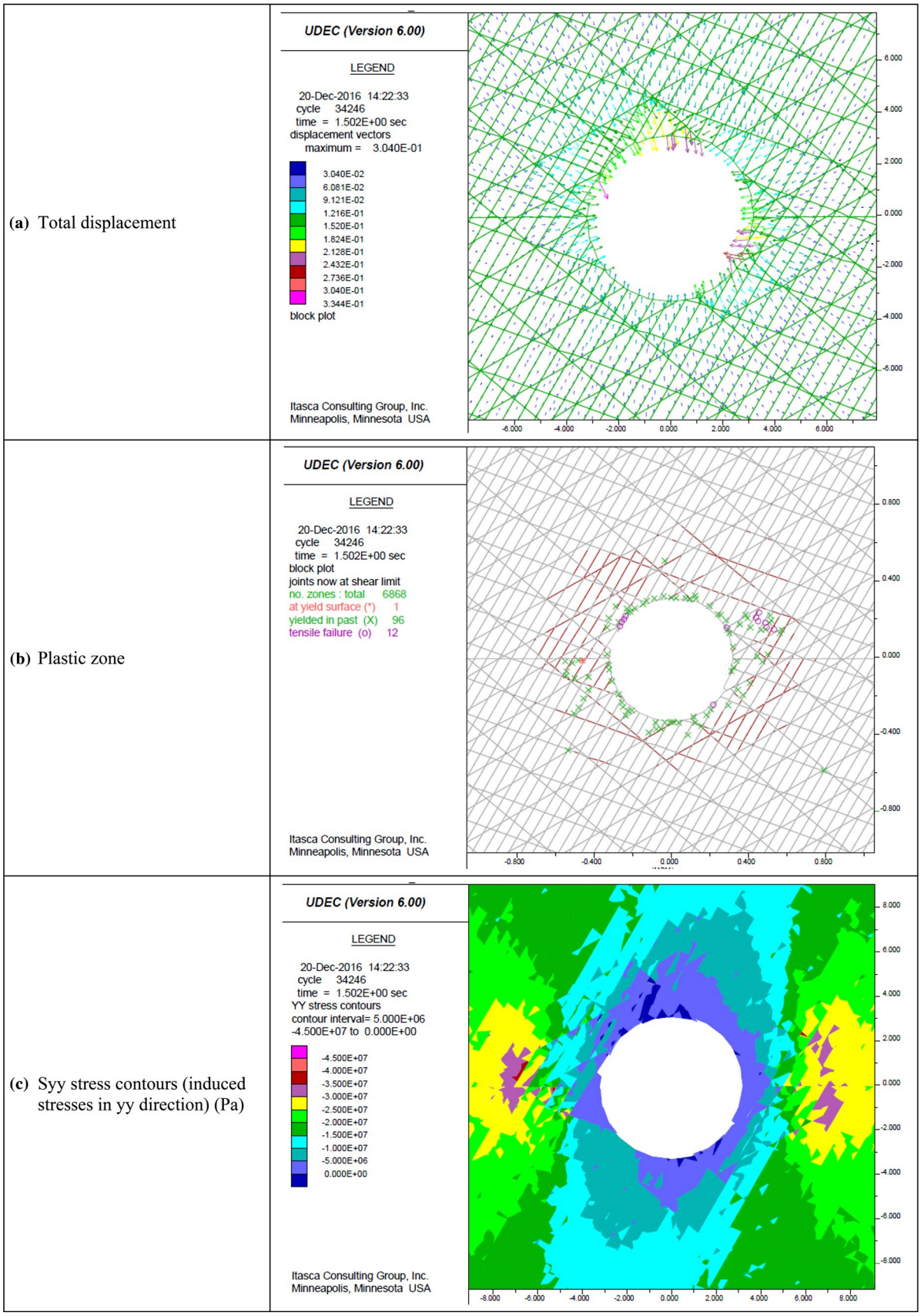

Fig. 6 Instability assessment parameters for DEM model for actual condition

adopted with regard to the displacement magnitude and depth of failure zone around the tunnel which is indicated in Table 5 (Solak 2009). According to the obtained results by discontinuous modelling, the ratio of displacement to tunnel radius is around 3.8%, and the ratio of depth of failure zone to tunnel radius is 1.04%. As indicated in Table 5, the blocky ground behaviour can be explained as deep-seated stress-induced failure.

5.3.3 Numerical Analysis in the Discontinuous Model with Emphasis on the In Situ Stress Effect

In this section, two other DEM models in lower in situ stress conditions are solved to prove the great effect of stresses around the tunnel on intensifying the extension of instabilities. The same procedure for the discontinuous model in Sect. 5.3.2 is followed except that the overburdens are defined as 100 and 400 m. According to the obtained results depicted in Fig. 7, the mean displacement for the tunnel with 100 m overburden is at around 6 mm, and the extension of failure zone is approximately 1 m. This gives out a negligible displacement percentage of 0.15% and a shear failure zone of 1.5 m without tensile failures. According to Table 5, the case with 100 m overburden goes into the category of stable ground. The other case at 400 m overburden with mean displacement of 5 cm and shear failure zone of 3.5 m without tensile failure provides displacement ratio of 1.5%. With regard to Table 5, the failure in the model can be specified as shallow stress-induced failure.

5.4 Analysing the Numerical Simulation Results

It can be inferred from the numerical simulations that the overall behaviour of the tunnel model is principally affected by the orientation and strength properties of discontinuities, as well as the high in situ stresses around the tunnel. Since the effect of slip failure on the joints cannot be considered by isotropic continuous models, realistic results are not anticipated in cases where joint sliding is the dominating factor (Solak 2009). In these cases, discontinuous models are more efficient.

By taking advantage of the results obtained from several numerical simulations, ground reaction curves (GRC) in continuous and discontinuous cases are compared. Then a rough estimation of the required thrust force for passing through the squeezing region is carried out. Additionally, an investigation is made upon the joint sets orientation as another effective factor to be considered in future studies.

5.4.1 Comparing the GRC in Different Modes of Analysis

It should be noted that a plain strain assumption is valid if the section under analysis is far from the tunnel face. Therefore, in order to compare the face regions ground behaviour in discontinuous and continuous models, the convergence–confinement method should be used to simulate the tunnel face effect by analysing the variations of internal pressure with tunnel convergence. As for the continuous model, specific amounts of internal pressure were applied on the tunnel wall in FLAC, and the resulting displacements were recorded. The obtained GRC is shown in Fig. 8. In order to validate this procedure, the same rock mass parameters were used in Carrenza Torres analytical equations (2004) to achieve the GRC. As can be seen, the results from numerical analysis are compatible with the ones from the analytical method. The same procedure was adopted in the DEM modelling using UDEC to evaluate the ground reaction to structural instabilities in the squeezing region at the 770 m overburden. Since there were numerous local blocky instabilities, the average displacements around the tunnel within a region with a 2 m thickness were used to evaluate the overall tunnel convergence. According to the diagrams in Fig. 8, large difference between results of continuous and discontinuous modelling can easily be perceived. For both discontinuous and continuous modes, the GRCs obtained from numerical method only cover the plastic mode of the rock mass, and the elastic mode with lower displacement and higher internal pressures was neglected.

5.4.2 Estimation of the Required Thrust Force of TBM to Advance Through the Squeezing Region

In order to assess the ground condition at the tunnel face and the shield–ground interaction to study the shield-jamming possibilities, advanced continuous three-dimensional models have been adopted recently (Hasanpour et al. 2014). However, in DEM modelling it is quite a new topic. Nevertheless, by accepting a degree of uncertainty,

Table 5 General categories of ground behaviour types (Solak 2009)

Behaviour type		Displacement/tunnel radius (displacement percentage)	Depth of failure zone/tunnel radius (failure percentage)
BT1	Stable ground	$<1\%$	0
BT3	Shallow stress-induced failure	$>1\%, <3\%$	<1.0
BT4	Deep-seated stress-induced failure	$>3\%$	>1.0

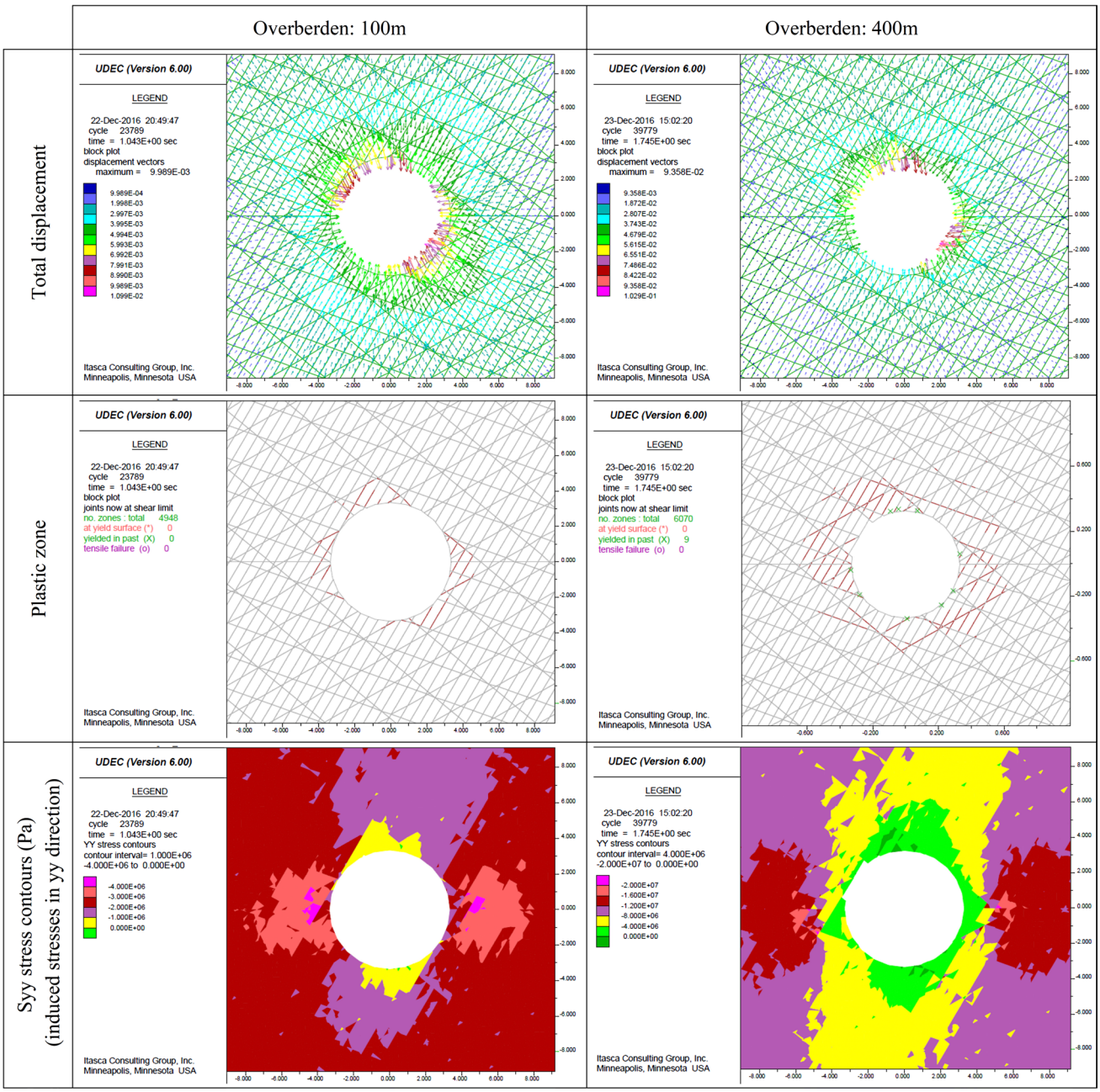

Fig. 7 Instability assessment parameters for DEM model

the convergence-confinement method can be employed in a simplified way to assess the ground behaviour in the vicinity of the tunnel face. According to Farrokh et al. (2006), the amount of applied pressure on the tunnel boundary is constant and can be divided into two components pertaining to the tunnel support system (shield) and the natural supporting pressure of the ground. The natural supporting pressure is the pressure that the tunnel face imposes on the tunnel perimeter due to the tunnel face effect. By using the longitudinal deformation profile (LDP) of the rock mass which indicates wall displacements at various distances from tunnel face, the locations where the shield interacts with surrounding rock can be specified. Subsequently, at different distances from the tunnel face, the imposed pressure of the ground on the shield can be evaluated. This amount can be estimated by subtracting the natural supporting pressure from the final pressure acting upon the support system at a distance far enough from the tunnel face (Farrokh et al. 2006).

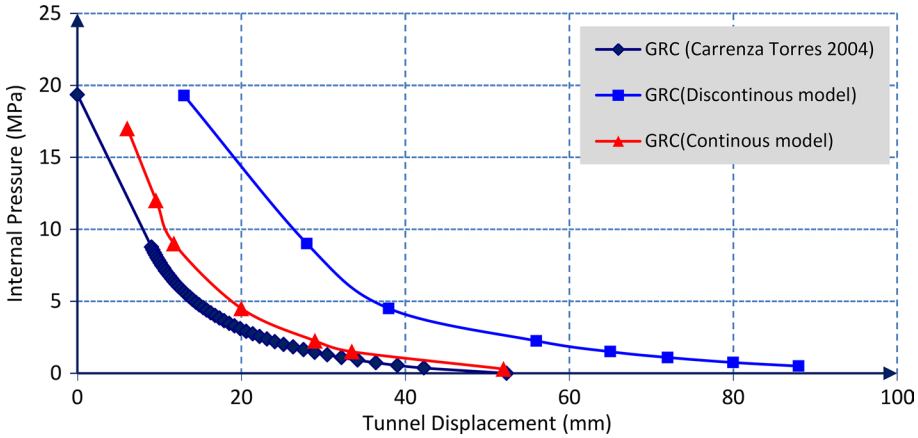

Fig. 8 Ground reaction curves obtained by different methods

In the squeezing region of the Zagros Tunnel, instead of common 17-inch gauge cutters of the TBM, larger 19-inch disc cutters were used to increase the overcutting gap between shield and rock. By this measure, a maximum value of 74 mm overcutting could be provided. However, a more realistic annular gap of 65 mm for possible wear on the disc cutters is considered in this study. Hence, after an initial displacement of 65 mm in front of the face, the shield will interact with the rock.

The LDP of the ground was simply obtained according to equations developed by Vlachopoulos and Diederichs (2009) by dint of plastic zone radius (Vlachopoulos and Diederichs 2009). It should be noted that more accurate LDPs should be achieved by using three-dimensional DEM simulations. As illustrated in Fig. 9, by considering the support characteristic curve (SCC) as a straight vertical line due to high stiffness of the shield as the support system, the final pressure on the shield can be approximately evaluated at 1.5 MPa. Moreover, 65 mm of displacement occurs at a distance of around 3.7 m from tunnel face. Since the shield length of TBM in the Zagros Tunnel is 12 m, the intersection of a vertical line from this position to the GRC can indicate the final ground pressure acting on the shield. This pressure is estimated by the following equation:

- Pi(at 12 m distance from face) = Pu-Pf(12 m) = 1.5 − 0.5 = 1 MPa
- Pu(x) = Final pressure acting on the support at a distance far enough from tunnel face (MPa)
- Pi = Ground pressure acting on the support at distance × from tunnel face (MPa)
- Pf(x) = Natural supporting pressure of ground at distance × from tunnel face (MPa)

By using this equation on a series of points on the shield, variation of ground pressures on the shield as a function of distance from tunnel face can be obtained as illustrated in Fig. 10. The integral of this diagram on the shield surface together with the TBM weight is applied to calculate the magnitude of the frictional forces imposed on the shield surface. As can be seen in Table 6, the total required thrust force for advancing through the squeezing region is approximately 54,277 kN. In this region, a thrust force of around 36,000 kN was applied by the auxiliary jacks of the TBM.

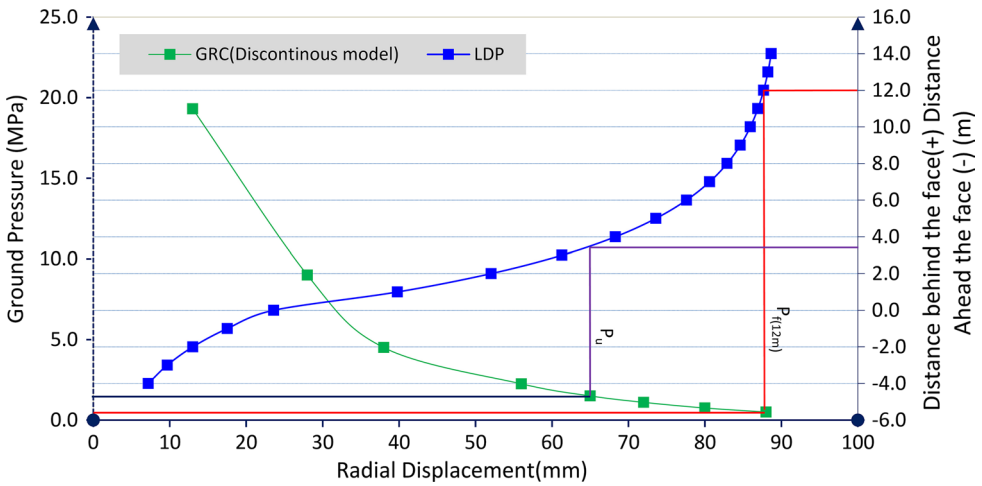

Fig. 9 Combination of GRC with LDP diagram to evaluate the ground pressure imposed on the support system

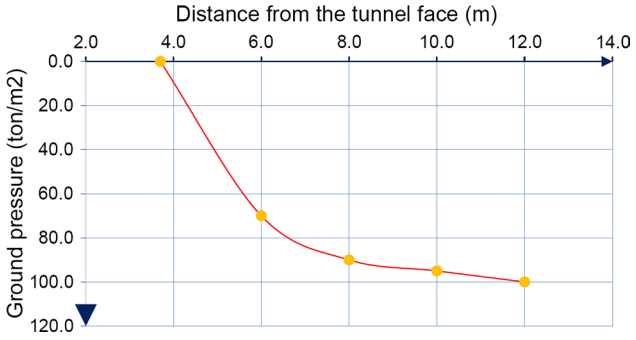

Fig. 10 Variation of ground pressure on the shield as a function of the distance from the tunnel face

Table 6 Total required thrust force for advancing through the squeezing region

Parameter	Value
Total ground pressure acting on the shield (ton)	13,000
Total TBM weight (ton)	573
Frictional force coefficient	0.4
Force at shield–rock interface (ton)	13,573
Total required thrust force (MN)	54.277 MN

But this amount was lower than the required thrust force and was not sufficient to compensate the frictional forces imposed on the shield–ground interface. One should bear in mind that more accurate estimations of pressure on the shield require further work on considering the effect of time during excavation by TBM.

5.4.3 The Effect of Joint Sets Orientation on the Tunnel Stability

An important parameter that can be included in the numerical modelling procedure is the effect of discontinuity strike, which should be considered with respect to the direction of tunnel axis. In order to facilitate the conclusion on whether the strike and dip are favourable or not, references are made to assessments of critical joint orientation effect by Bieniawski (1989). The derived results are inserted in Table 7. According to the data, the bedding plane and Joint Set 1 with the lowest joint spacing have unfavourable and very unfavourable conditions, respectively. This fact proves the necessity of sufficient understanding upon discontinuity strike that can be assessed in more accurate three-dimensional DEM modellings in the future.

6 TBM Shield-Jamming Condition

The excavation operation in the Zagros Tunnel was accompanied by numerous problems when the TBM started excavation in JL5 unit. While boring through the chainage 18 + 498 km to 18 + 546 km in 7 July 2014, the TBM encountered difficulties in argillaceous limestone with interlayers of shale (in JL5 formation) with an approximate tunnel overburden of 770 m. Consequently, the TBM was jammed in the back and front shield and was incapable of resuming excavation through the path. According to the recorded data, the utilization factor (UF) of TBM reached the average percentage of 16.1% from the onset of boring through this unit in March 2014 until the end of excavation in September 2014. In July 2014, the minimum UF of 7% was recorded. In Fig. 11, the lithological condition in the tunnel path and the TBM jamming section are illustrated schematically. Figure 12 shows pictures of the machine being entrapped by the ground. A diagram containing the tunnelling time consumption distributed on various operations in July 2014 is shown in Fig. 13.

7 Actual Consequences of Encountering Squeezing Ground

In mechanized tunnelling, squeezing risks can be identified and spotted by relevant symptoms. As a result, monitoring the situation and seeking such indications could make a great contribution to the engineers and working staff to get informed of potential risks and accordingly avoid the TBM jamming. These symptoms can be recognized in three separate divisions including geological indications, influences on

Table 7 Assessment of critical joint orientation effect (Bieniawski 1989)

Joint sets	Joint spacing (m)	Orientation		Condition
		Apparent dip angle	Strike	
Bedding plane	1.50	30	170 (perpendicular to tunnel axis)	Unfavourable
Jl	0.55	60	50 (parallel to tunnel axis)	Very unfavourable
J2	2.50	40	50 (parallel to tunnel axis)	Fair
J3	1.75	20	145 (perpendicular to tunnel axis)	Favourable

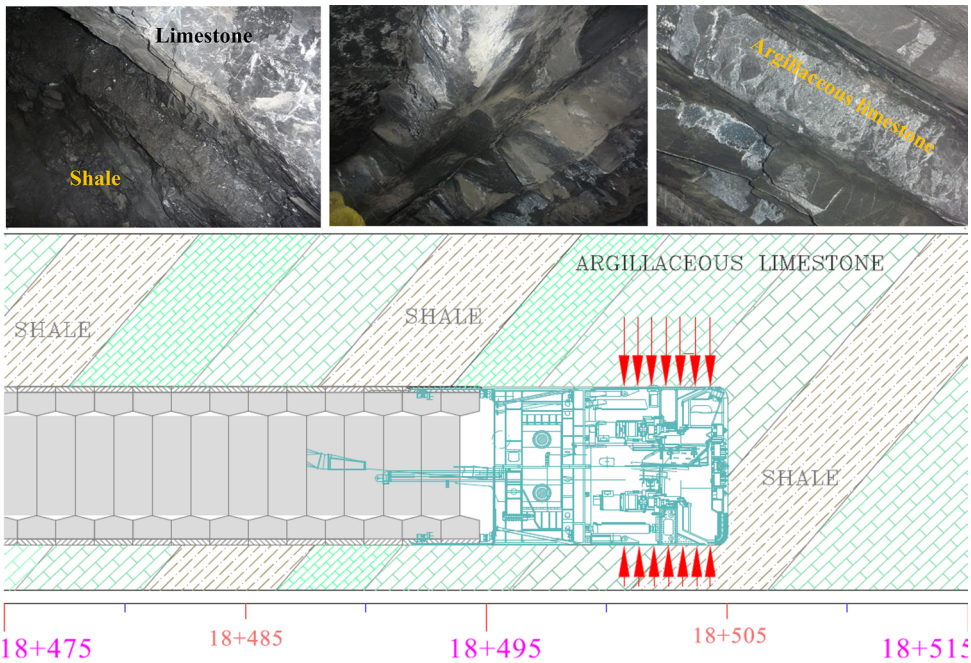

Fig. 11 Position where TBM was jammed in JL5 unit

Fig. 12 A number of pictures of the ground convergence and the TBM getting entrapped

the tunnel lining as well as effects on the TBM performance parameters.

7.1 Geological Indications

Monitoring the geological conditions during excavation can be regarded as one of the most important and fundamental steps in recognizing ground behaviour and identifying excavation hazards. Since the ground could exhibit different behaviours in different hazardous states, the geological conditions should be frequently monitored by engineering geologists with acceptable accuracy.

Squeezing hazards can often be monitored by the amount of injected pea gravel and cement grouting as

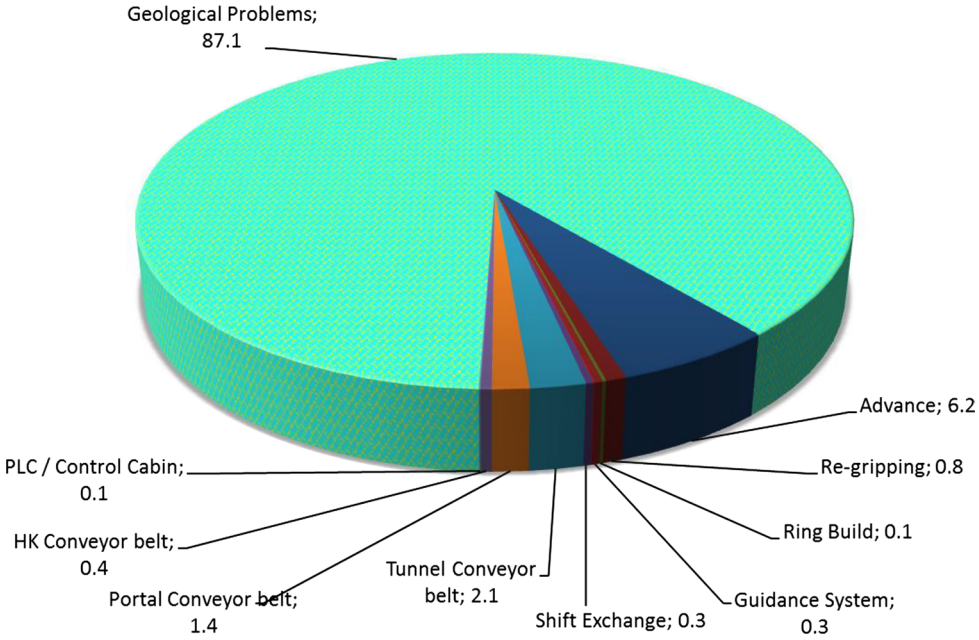

Fig. 13 Tunnelling time consumption distributed on various operations in July 2014

backfill materials behind the segmental lining. Due to excessive convergences, the gap between segmental lining and tunnel wall decreases, and consequently, pea gravel and cement grouting injection operation is hindered or becomes impossible. These consequences are good indicators of squeezing ground. It should be noted that in local blocky crushed zones, the same overall evidence is anticipated; however, in these cases, pea gravel injections and cement grouting volumes are not uniformly distributed around the tunnel perimeter. In other words, for local blocky crushed zones, uneven volumes of injected pea gravel and cement grouting are anticipated in different points of the tunnel perimeter, whereas more even distributions are expected for squeezing conditions.

As a rule, when TBM passes through squeezing regions of the Zagros Tunnel, two main consequences including sharp drops in pea gravel and cement grouting injection volume are likely to occur. The backfill volume including pea gravel and cement grouting injections for a 200 m length of tunnel in the chainage 18 + 400 km to 18 + 600 km is indicated in Fig. 14.

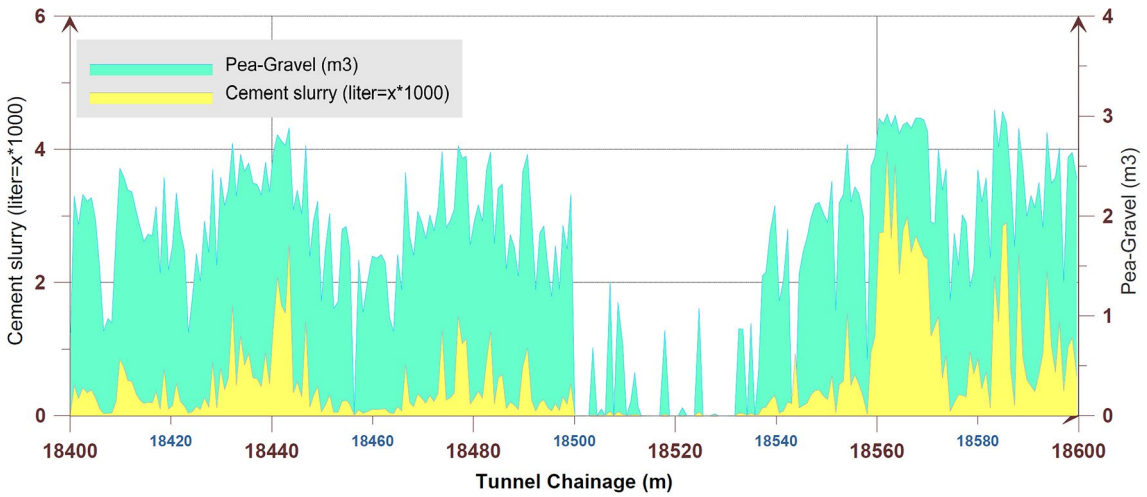

Fig. 14 Segmental lining backfilling injection volume for pea gravel and cement grouting (chainage 18 + 400 km to 18 + 600 km)

7.2 Influence on the Tunnel Lining

Due to potential cracks and even aggravating failure of the segmental lining in critical cases of squeezing conditions, it is essential to consider the deleterious squeezing loads in the lining structural design process.

Other evidences associated with the onset of squeezing conditions in the Zagros Tunnel were the signs of time-dependent failure reflected in segmental lining while passing through the JL5 unit. These signs were observed in the form of initiated cracks in the roof and the right wall segments in the chainage of 18 + 498 km to 18 + 546 km. From the geometric point of view, the cracks were mostly longitudinal and inclined to some extent with apertures of 0.5 to 6 mm which were formed in the centre of segments and parallel to the tunnel axis. Some of the formed cracks on a number of roof segments are indicated in Fig. 15.

7.3 Influence on the TBM Performance Parameters

7.3.1 Thrust Forces and Cutterhead Torque

In mechanized excavation, TBM performance parameters are among other factors which are strongly affected by ground conditions. Data logging and appropriate interpretations on them could make a great contribution to proper understandings upon ground behaviour. In the Zagros Tunnel, intermittent limestone and shale layers with different strength parameters resulted in irregular changes in TBM performance parameters in JL5 unit. The majority of these changes were recorded as more thrust force and less torque magnitudes in limestone compared to shale. But the variation rates of these parameters in squeezing regions were noticeable. The variation of thrust force, torque and power values for the zone with 200 m length was recorded by the machine data logger in the Zagros Tunnel.

The obtained data are illustrated through corresponding diagrams in Fig. 16. It can be deduced that there has been a significant rise in the thrust force in chainage 18 + 498 km to 18 + 546 km, while no considerable changes in torque and power of machine were identified in this region. The same situation with a slight difference can be observed in chainage 18 + 445 km to 18 + 470 km in which the first TBM jamming occurred.

7.3.2 Field Penetration Index (FPI)

Field Penetration Index (FPI) was introduced by Nelson et al. (1983), and it was subsequently applied to TBM performance prediction. Some of the most important performance parameters, including average penetration rate (ROP), penetration per revolution (P) and Field Penetration Index (FPI), have been estimated according to the following formula (Klein et al., 1995; Barton, 2000; Gong and Zhao 2007).

$$\mathrm{FPI} = F_n/P = \left[(60 \times F_n \times \mathrm{RPM})/(1000 \times \mathrm{ROP})\right]$$

where F_n is average cutter load (kN/cutter), P is penetration rate (mm/revolution), RPM is cutterhead speed (revolution per minute) and ROP is penetration rate (m/h).

In squeezing regions, FPI is considered as one of the most practical variable parameters of TBM. Increasing the thrust force of the machine in squeezing regions could raise the FPI in each stroke. This rise in the thrust force is the consequence of two occurrences including (a) the ground movement and (b) the pressure imposed by the tunnel face to the cutterhead as well as the attempts made by the operator to counteract this condition and keep pace with it in order to maintain the penetration rate and avoid TBM jamming. From this evidence, it can be simply inferred that the escalation

Fig. 15 Formation of longitudinal cracks in roof segments in the chainage 18 + 498 km to 18 + 546 km

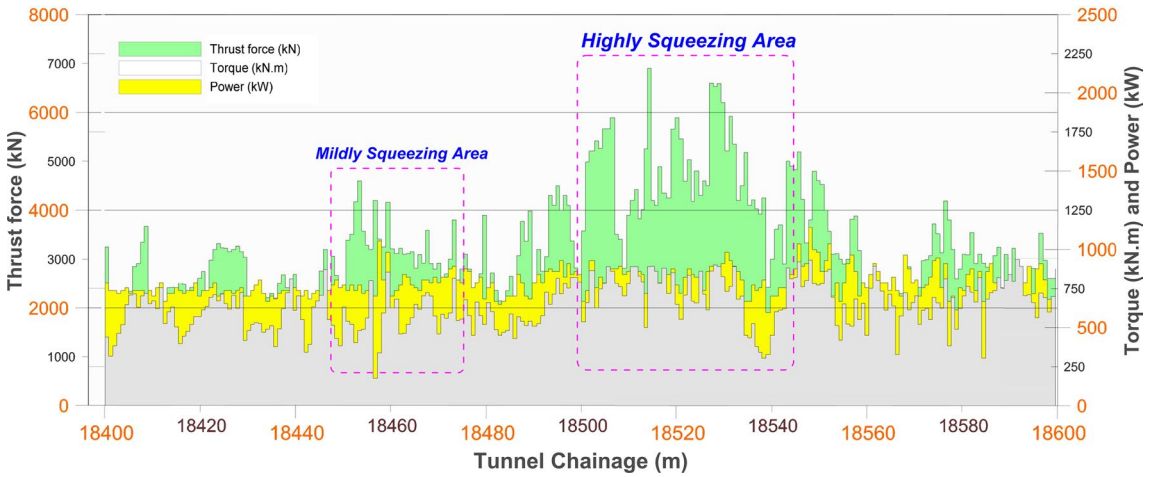

Fig. 16 Variation of TBM performance parameters in the chainage 18 + 400 km to 18 + 600 km

in FPI with respect to constant penetration rate (PR) could be interpreted as one of the most significant symptoms of squeezing ground reflected in performance parameters.

In Fig. 17, the variations of thrust force, penetration rate (PR) and FPI have been indicated through corresponding diagrams. It can be deduced from this figure that in the squeezing region, for specific constant values of PR, there has been a noticeable rise in the thrust force and the resulting FPI. Besides, Fig. 17 shows the relationship between FPI and the volume of injected segment backfill material (pea gravel and cement grouting) for the chainage 18 + 400 km to 18 + 600 km.

Conducted investigations on the obtained results of FPI with respect to the volume of injected backfilling material (pea gravel and cement grout) for the squeezing region demonstrates that these two indices have acceptable relationships and verify the two sections with squeezing hazards (Fig. 18).

7.3.3 Pressure of Auxiliary Thrust Cylinder Jacks

In addition to the applied thrust jacks in double-shield machines, auxiliary jacks are also installed with one end attached to the gripper shield and the other end supported by the last segments. These jacks impose pressure to the last installed segment and push the shield towards the tunnel face. The auxiliary jacks provide the machine with two common modes of excavation including single mode and double mode also known as gripper mode. The single-mode excavation technique is introduced as one of the principle pragmatic approaches for passing through squeezing regions. In this technique, two main procedures are followed. Thrust jacks are completely disabled, and the telescopic shield part of the machine gets closed. Consequently, the excavation process is conducted discontinuously with frequent excavation and segment installation

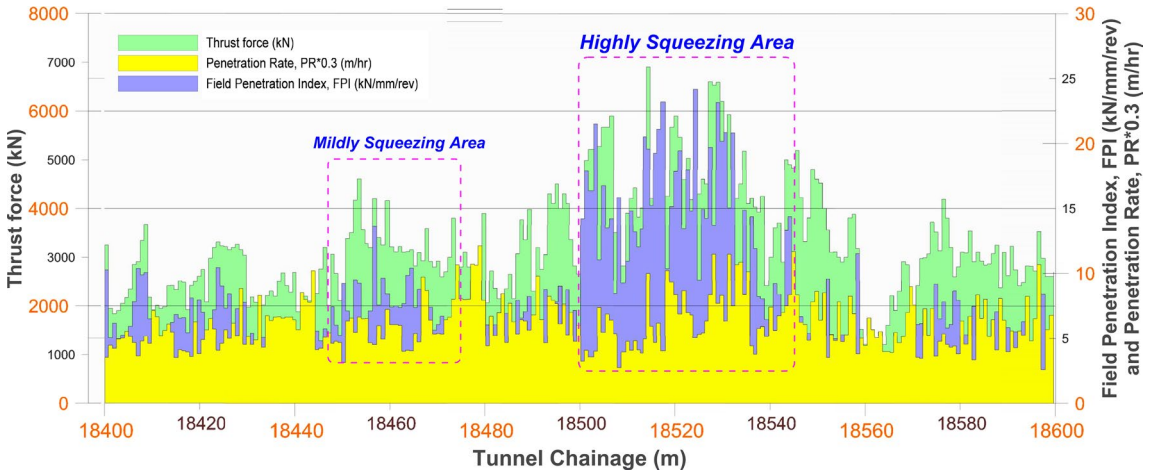

Fig. 17 Variation of thrust force, penetration rate (PR) and FPI of the TBM in the chainage 18 + 400 to 18 + 600 km

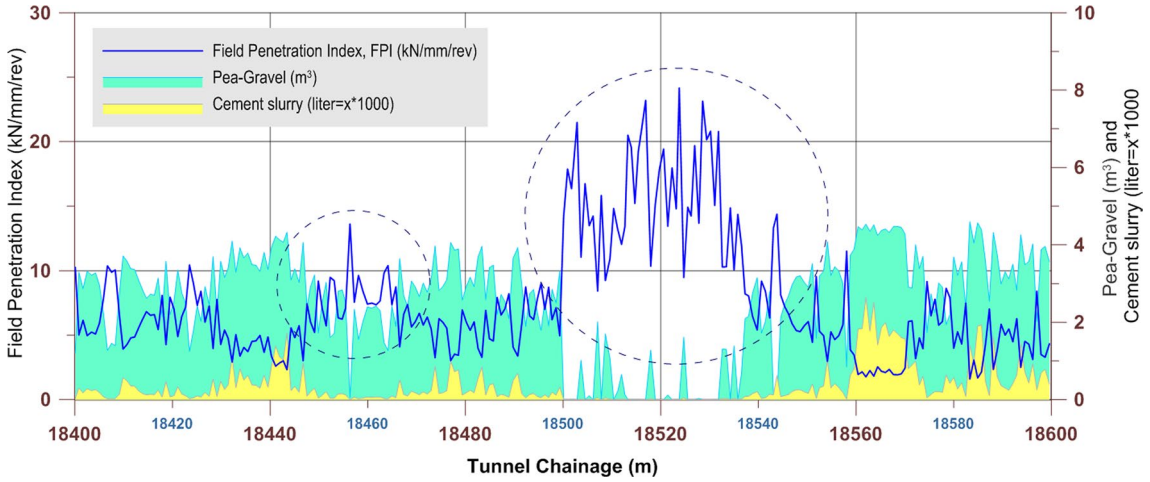

Fig. 18 Relationship between Field Penetration Index (FPI) with the observed geological evidences in the chainage 18 + 400 to 18 + 600 km

processes. Under these circumstances, the TBM advances only by means of auxiliary jacks.

Due to the capability of single-mode excavation in reducing the contact area between the machine and squeezing ground, this technique is regarded as an efficient method for passing through the squeezing regions. In this project, attempts were made to implement this approach in order to advance through the critical areas. This facilitated TBM advance through slightly squeezed regions in the chainage 18 + 445 km to 18 + 470 km; however, it was not successful in the chainage 18 + 498 km to 18 + 546 km due to excessive ground convergences. The imposed pressure on the auxiliary jacks exceeded the mean value of 90 bar. Lastly, the TBM was completely jammed in 18 + 504 km, and subsequent attempts in increasing the pressure up to the noticeable value of 400 bar failed to release the machine. The variation of imposed pressure on the auxiliary jacks for the Zagros Tunnel is depicted by a diagram in Fig. 19.

8 The Main Strategies for Releasing the TBM

8.1 Introducing

Taking suitable measures for releasing the TBMs in squeezing regions has attracted a great deal of attention among tunnelling engineers. These releasing approaches should be practical, cost and time effective and above all have an acceptable level of safety. In this section of the research, actual experiences gained through the TBM releasing operation of the Zagros Tunnel are described step by step.

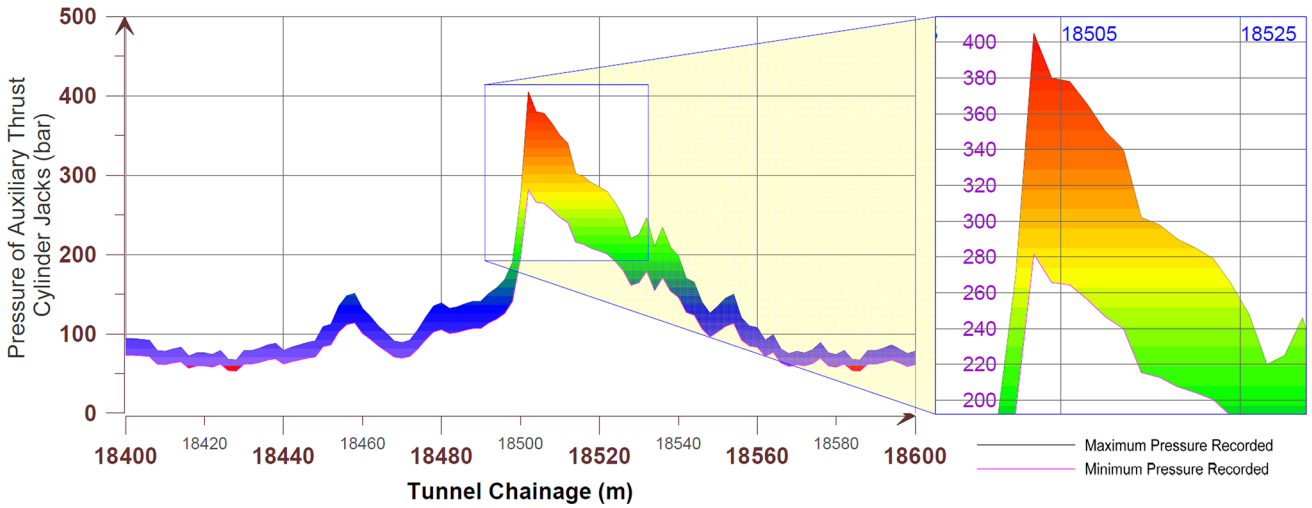

Fig. 19 Diagram indicating variation of imposed pressure on the auxiliary jacks in the chainage 18 + 400 km to 18 + 600 km

8.2 Getting Access to the Other Side of the TBM Shield

Detailed observations through the existing openings in the shield demonstrated that the machine was entrapped by the ground in the area between the tail shield and the cutterhead. Hence, attempts were made to provide enough space behind the shield so as to excavate the surrounding rocks. To fulfil this objective, the last installed roof segment in the tail shield area was removed, and after releasing the auxiliary jacks, a window with dimension of 60 cm × 80 cm was cut through the upper right part of the tail shield (Fig. 20).

8.3 The Excavation Method of Rescue Gallery

Due to special conditions in the jammed sections of this project, two general excavation methods including mechanical and blasting techniques were compared from safety and operation points of view. The disadvantages of blasting method together with advantages pertaining to mechanical excavation method are explained as follows:

Disadvantages of blasting method:

- Extension of plastic zone in the rock mass surrounding the TBM and aggravating the planes situation around the tunnel.
- Escalation in support system costs due to extension of plastic zone.
- Possible damages to the TBM shield.
- Time-consuming operations which require blasting specialists as well as necessity of building warehouses for storage of explosive materials.

Advantages of mechanical excavation:

- Time effective operations.
- No need for a wide excavation face.
- A controlled excavation process with minimum damage to the surrounding rock mass.
- Less damage to the TBM shield.
- Quick and easy access to the required mechanical excavation equipment including rock drilling hammers, pneumatic and commissioning systems.

With regard to the existing 770 m overburden and rock masses containing intermittent layers of limestone and shale and the aforementioned notes, the mechanical excavation by rock drilling hammers was suggested. Pictures taken from the applied equipment for releasing the TBM in the Zagros Tunnel are illustrated in Fig. 21.

Since the TBM was completely entrapped by the rock mass, in the first step a rescue gallery was excavated in the area between tail shield and cutterhead. The height and width of the gallery are 0.8 and 2 m, respectively. In the next step, the gallery was used to excavate the sides of the shield (see Figs. 22, 23)

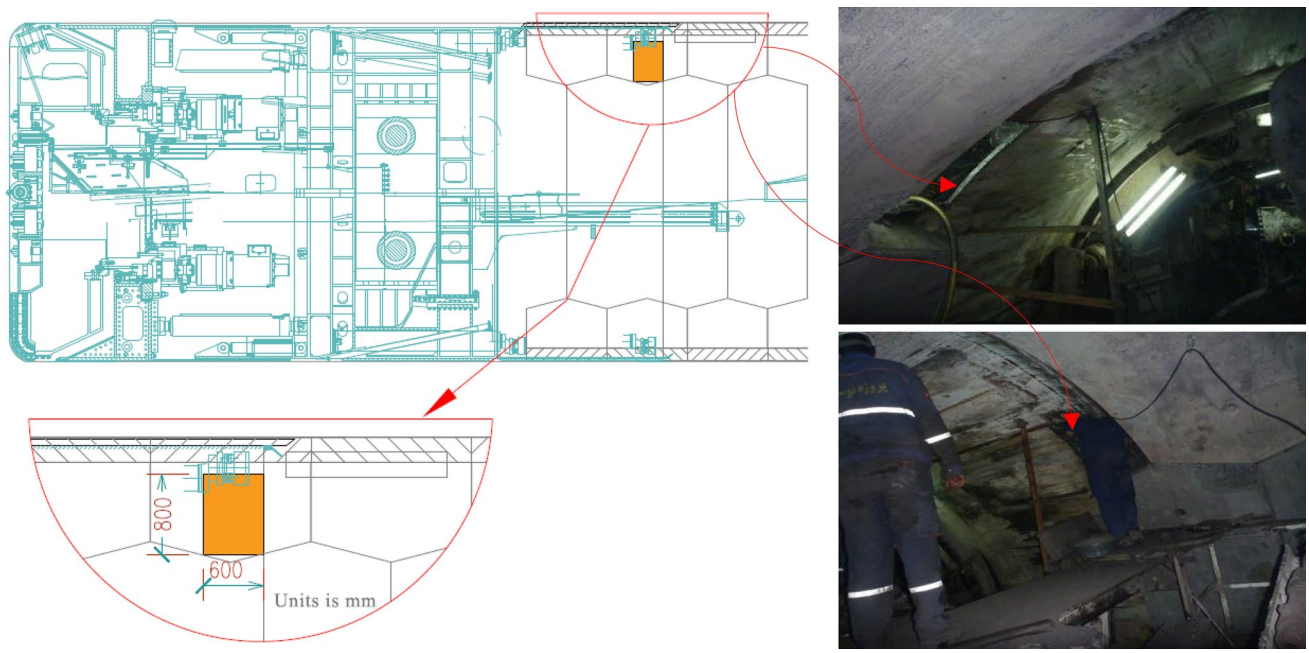

Fig. 20 Cutting position in the tail shield to access the surrounding rock mass

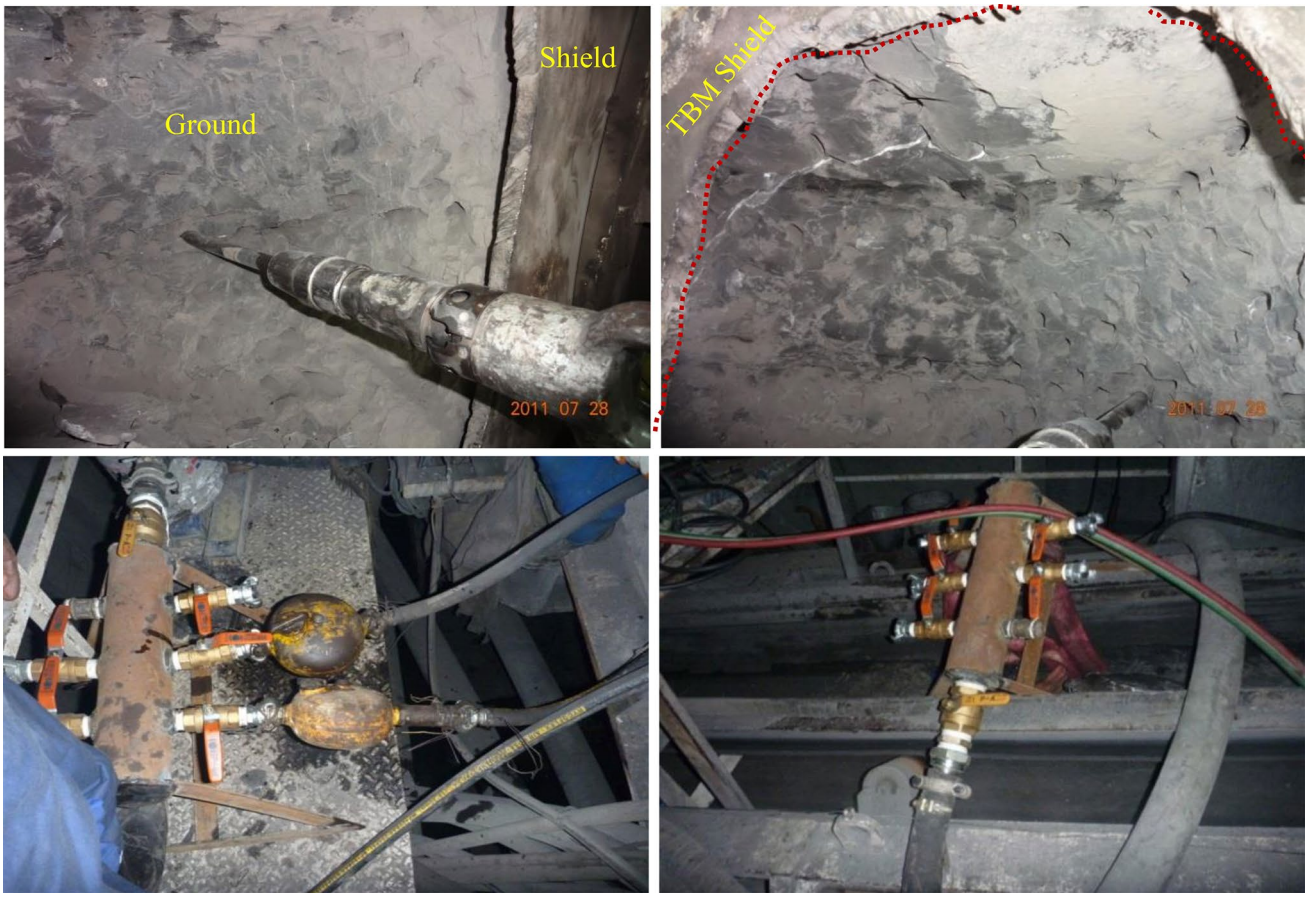

Fig. 21 Pictures taken from the applied equipment for releasing the TBM in the Zagros Tunnel

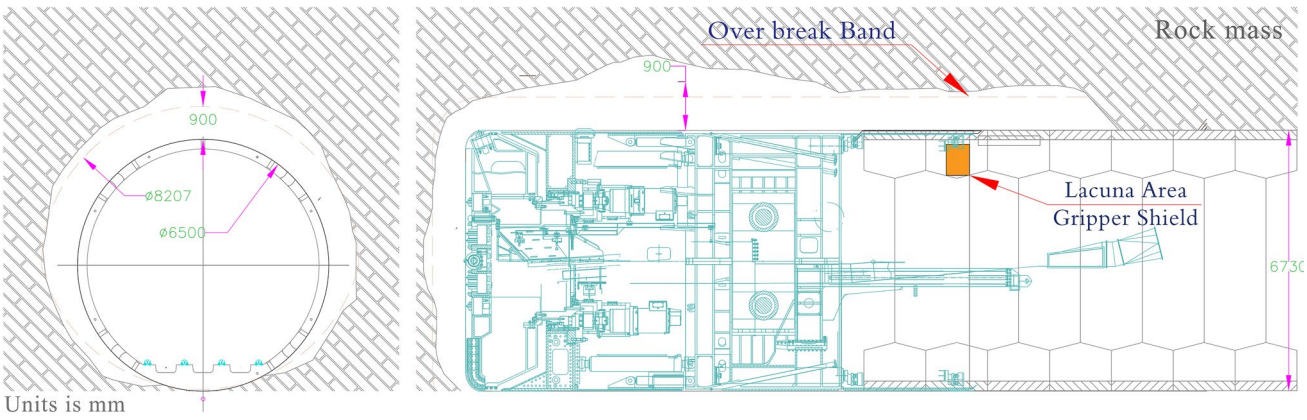

Fig. 22 A schematic illustration of the position of gallery used to release the TBM

8.4 Support System of the Gallery

After releasing the sides of the TBM shield, it was necessary to support the gallery due to the weak rock mass especially in regions containing shale (due to the humidity and quick weathering of the shale formation) and in argillaceous limestone (because of structural failures in joint sets with unfavourable orientation). The support systems must be quickly and easily installed during the releasing operation to provide safety for the workers.

For this purpose, by considering the available equipment, the necessity for quick installation of the support

Fig. 23 Excavation operation and the gallery in right and upper side of the front shield

system and the orientation of rock mass joint sets, timbers were proposed for the temporary support system. The timbers were installed on the shield with a spacing range of 0.4–0.8 m to transfer the load imposed by the ground. The installed timbers with the structural condition of the squeezing region are depicted in Fig. 24.

8.5 Injecting High-Expansion Foams for Filling Purposes

Excavating the surrounding rock mass increased the perimeter of the excavation section compared to its initial perimeter bringing about a larger gap between tunnel wall and shield. This gives rise to two main limitations in the machine advance through this region:

- The installed timbers get toppled and subsequent collapse of the rock mass and blocks on the shield could once again lead to jamming of the machine.
- The installation of the segmental lining gets hindered. Indeed, wall segments will fall into the gap and the roof segment could consequently topple.

Therefore, the produced gap between TBM shield and the tunnel wall needs to be filled with suitable filler materials. In this project, polyurethane high-expansion foams were used and the existing gap especially in the tunnel roof was filled up. This operation was repeatedly carried on until the machine passed through the squeezing region.

8.6 Special Precautionary Measures for Boring Through the Squeezing Region

To summarize, some particular precautionary measures were taken by operational staff which made a great contribution to the excavation process while boring through squeezing regions. These experiences can be employed for further exercises in similar cases:

- Continuous and steady excavation without pause.
- Applying 19-inch gauge cutters instead of the original 17-inch cutters to increase the overcutting space around the tunnel.
- Employing single-shield excavation mode in the critical regions.
- Injecting two-component foams to stabilize the collapsed blocks in front of the cutterhead prior to excavating the gallery in the cutterhead area (see Fig. 25).
- Injecting oil and grease as lubricants to reduce the frictional forces between shield and rock through a number of installed hoses for each two excavation strokes.

Figure 25 shows two-component foams injected through the collapsed blocks in front of the cutterhead.

Fig. 24 Timbers used to facilitate the TBM releasing operation

Fig. 25 Two-component foams injected through the collapsed blocks in front of the cutterhead

9 Conclusion

The double-shield TBM of the Zagros Tunnel was jammed on 6 July 2014 while boring through the medium bedded argillaceous limestone with interlayers of shale (JL5 formation) in an overburden of 770 m. Subsequent drastic measures in increasing the pressure of auxiliary cylinder jacks to the noticeable value of 400 bar failed to release the machine. In order to analyse the situation, numerical continuous and discontinuous simulations were conducted in the shield-jamming section. Results demonstrated that the discontinuous numerical analysis was more compatible with the ground actual state in the region. However, through further investigations in this field, the realistic rock mass parameters to be applied in equivalent continuous models could be calibrated by trial and error in the numerical process.

It was proved that excavating through the rock mass with high in situ stresses consisting of various unfavourable joint sets triggers stress relaxation and consequently entraps the TBM. In addition to the theoretical analysis, the experiences gained through the Zagros Tunnel indicate that taking advantage of geological observations, controlling and monitoring the segmental lining and analysing the performance parameters of TBM are regarded as chief techniques to identify the onset of squeezing in mechanized tunnelling. Besides, it was concluded that continuous excavation in single mode, using larger-diameter gage cutters and injecting lubricants to decrease the frictional forces are among major technical measures that can be taken in squeezing regions with jamming potential to avoid subsequent TBM downtime.

Acknowledgments The authors would like to express their gratitude to HARAZRAH Consulting Engineers Group for providing the facilities for the authors and a special thanks to Mr. H. Pourmoghaddam for his help in preparing the database.

References

Barla G (2001) Tunnelling under squeezing rock conditions. Eurosummer-school in tunnel mechanics, Innsbruck. Logos Verlag, Berlin, pp 169–268

Barla G, Pelizza S (2000) TBM tunnelling in difficult ground conditions. GeoEng, Melbourne, Australia

Barton N (2000) TBM tunnelling in jointed and faulted rock. Balkema, Rotterdam

Bieniawski ZT (1989) Engineering rock mass classifications. Wiley, New York, p 251

Bilgin N, Algan M (2012) The performance of a TBM in a squeezing ground at Uluabat, Turkey. Tunn Undergr Sp Technol 32:58–65

Farrokh E, Mortazavi A, Shamsi Gh (2006) Evaluation of ground convergence and squeezing potential in the TBM driven Ghomroud tunnel project. Tunn Undergr Space Technol 21:504–510

Ferrero AM, Migliazza M, Giani GP (2004) Analysis of tunnel stability comparison between continuous and discontinuous approaches. In: SINOROCK2004 symposium. Int J Rock Mech Min Sci 41(Suppl. 1):646–651

Goel RK, Jethwa JL, Paithakan AG (1995) Tunnelling through the young Himalayas—a case history ofthe Maneri-Uttarkashi power tunnel. Eng Geol 39:31–44

Gong QM, Zhao J (2007) Influence of rock brittleness on TBM penetration rate in Singapore granite. Tunn Undergr Sp Technol 22:317–324

Goricki A, Button EA, Schubert W, Potsch M (2005) The influence of the discontinuity orientation on the behavior of tunnels, Felsbau 5. VGE Essen, pp 12–18

Hasanpour R, Rostami J, Ünver B (2014) 3D finite difference model for simulation of double shield TBM tunneling in squeezing grounds. Tunn Undergr Space Technol 40:109–126

Hoek E, Marinos P (2000a) Predicting tunnel squeezing problems in weak heterogeneous rock masses. Tunn Tunn Int 32(11):45–51

Hoek E, Marinos P (2000a) Predicting tunnel squeezing problems in weak heterogeneous rock masses. Tunnels and Tunnelling International Part 1: 45–51

Hoek E, Marinos P (2000b) Predicting tunnel squeezing problems in weak heterogeneous rock masses. Tunnels and Tunnelling International Part 2: 33–36

Itasca, FLAC2D (2013) Version 7 users manuals. Itasca Consulting Group, Minneapolis, NM

Itasca, UDEC (2013) Version 6 users manuals. Itasca Consulting Group, Minneapolis, NM

Jethwa JL, Singh B, Singh B (1984) Estimation of ultimate rock pressure for tunnel linings under squeezing rock conditions-a new approach. In: Proceedings of the ISRM symposium on design and performance of underground excavations, Cambridge, UK, September 3–4

Klein S, Schmoll M, Avery T (1995) TBM performance at four hard rock tunnels in California. In: Proceedings of the rapid excavation and tunnelling conference, pp 61–75 (Chapter 4)

Leitner R, Potsch M, Schubert W (2006) Aspects on the numerical modelling of rock mass anisotropy in tunneling. Felsbau 2:59–65

Mahendra S, Bhawani S, Jaysing Ch (2007) Critical strain and squeezing of rock mass in tunnels. Tunn Undergr Space Technol 22:343–350

Maria F, Maria M, Paolo GG (2004) Analysis of tunnel stability: comparison between continuous and discontinuous approaches. Int J Rock Mech Min Sci 41:646–651

Narimani Dehnavi R, Sadeghi M, Baradaran E, Ebrahim MB (2016) The performance of a TBM in difficult ground conditions of Golab water transfer tunnel: a case study in Iran. In: Proceedings of 2nd international conference on tunnel boring machines in difficult Grounds, Turkey

Nelson P, O'Rourke TD, Kulhawy FH (1983) Factors affecting TBM penetration rates in sedimentary rocks. In:. Proceedings of 24th US symposium on rock mechanics, Texas A&M, College Station, TX, pp 227–237

Panthi KK (2006) Engineering geological uncertainties related to tunnelling in Himalayan rock mass conditions. Ph.D. Thesis

Panthi KK, Nilsen B (2007) Uncertainty analysis of tunnel squeezing for two tunnel cases from Nepal Himalaya. Int J Rock Mech Min Sci 44:67–76

Ramoni M, Anagnostou G, (2006) On the feasibility of TBM drive in squeezing ground. In: ITA world tunnelling congress, safety in underground space, COEX, Seoul, South Korea, pp 1–15

Ramoni M, Anagnostou G (2010a) Tunnel boring machines under squeezing conditions. Tunn Undergr Space Technol 25:139–157

Ramoni M, Anagnostou G (2010b) Thrust force requirements for TBMs in squeezing ground. Tunn Undergr Space Technol 25(4):433–455

Ramoni M, Anagnostou G (2011) The interaction between shield ground and tunnel support in TBM tunnelling through squeezing ground. Rock Mech Rock Eng 44:37–61

Rasouli Maleki M (2009) Engineering geological studies of the diversion tunnel, focusing on stabilization analysis and support design, Iran. Engineering Geology 108:208–224

Rasouli Maleki M (2011) Study of the engineering geological problems of the Havasan Dam, with emphasis on clay-filled joints in the right abutment. Rock Mech Rock Eng 44:695

Rasouli Maleki M (2018a) Groundwater Seepage Rate (GSR); a new method for prediction of groundwater inflow into jointed rock tunnels. Tunn Undergr Space Technol 71:505–517

Rasouli Maleki M (2018b) Rock Joint Rate (RJR); a new method for performance prediction of Tunnel Boring Machines (TBMs) in hard rocks. Tunn Undergr Space Technol 73:261–286

Rasouli Maleki M, Memmarian M (2015) Stability analysis of muck-car tipper cavern use to UDEC numerical program. In: 11th Iranian and 2nd regional tunnelling conference, Tehran, Iran

Rasouli Maleki M, Yousefi Mahmoud N (2015) Detection of hydrogen cyanide (HCN) gas in tunnels and fundamental strategies to deal with it. Environ Earth Sci 74(9):6919–6927

Shaterpour Mamaghani A, Tumac D, Avunduk E (2015) Double shield TBM performance analysis in difficult ground conditions: a case study in the Gerede water tunnel, Turkey. Bull Eng Geol Eviron 75(1):251–262

Singh B, Goel RK (2006) Tunneling in weak rocks, 5th edn. Elsevier, London

Singh B, Jethwa JL, Dube AK, Singh B (1992) Correlation between observed support pressure and rock mass quality. Tunn Undergr Space Technol 7(1):59–74

Solak T (2009) Ground behavior evaluation for tunnels in blocky rock masses. Tunn Undergr Space Technol 24:323–330

Stead D, Eberhardt E, Coggan J, Benko B, (2001) Advanced numerical techniques in rock slope stability analysis—applications and limitations. In: International conference on landslides-causes, impacts and countermeasures, pp 615–624

Vlachopoulos N, Diederichs MS (2009) Improved longitudinal displacement profiles for convergence confinement analysis of deep tunnels. Rock Mech Rock Eng 42(2):131–146